Nucleic Acids Research, 1993, Vol. 21, No. 16 3857–3865

Intracellular disposition and metabolism of fluorescently-labeled unmodified and modified oligonucleotides microinjected into mammalian cells

Tracey L.Fisher+, Terry Terhorst, Xiaodong Cao and Richard W.Wagner*
Gilead Sciences, 346 Lakeside Drive, Foster City, CA 94404, USA

Received March 10, 1993; Revised and Accepted June 9, 1993

ABSTRACT

The intracellular distribution and metabolism of microinjected fluorescently-labeled oligonucleotides (ODNs) have been evaluated using confocal fluorescence microscopy. Fluorescent phosphodiester ODNs, microinjected into the cytoplasm of mammalian cells, rapidly accumulate within the nucleus; the fluorescence disappears with a half-life of 15–20 minutes. Microinjected fluorescent phosphorothioate ODNs remain in the nucleus for more than 24 hours. The persistence of fluorescence depends on the length of the ODN. Modification of the 3′ end of phosphodiester ODNs does not significantly slow the rapid disappearance of fluorescence, although certain 3′ modifications localize ODNs into the cytoplasm. Using specially designed ODNs, endonuclease activity is demonstrated to exist in the cytoplasm and nucleus. Modification of the 2′ position of the ribose rings of a fluorescent phosphodiester oligodeoxynucleotide with *O*-methyl or *O*-allyl does not alter its intracellular distribution; however, the 2′-*O*-allyl modification stabilizes the persistence of fluorescence more than 60-fold compared to the 2′-deoxy control. Thus, the experiments indicate that somatic cells contain nucleolytic activities which degrade microinjected ODNs; however, chemical modification can dramatically circumvent this process.

INTRODUCTION

Development of antisense oligonucleotides (ODNs) has focused on modifications which satisfy three conditions for improved efficacy: (*i*) stability to serum and cellular nucleases, (*ii*) enhanced cellular permeability, and (*iii*) high affinity, sequence-specific interaction with target RNA. The presence of nucleases within cells, coupled with poor cellular permeability of ODNs, may account for the high dose concentrations needed to achieve biological effects attributable to sequence-specific antisense gene inhibition. Several recent reports and reviews discuss the effects of ODN modifications on nuclease stability, cellular permeability, and binding affinity (1–7).

Given the problems outlined above, the fate of ODNs in serum and within cells has become a pressing question in the antisense field. Two types of methods have been used to address ODN intracellular localization and metabolism in mammalian cells: fluorescence microscopy, using fluorescently-labeled ODNs, and cell fractionation, using radioactive ODNs. Fluorescent and radioactive cellular uptake results suggest that ODNs associate with cells and enter the cytoplasm through endocytosis (8, 9) where they remain mostly undegraded (10, 11), especially if they are modified at the 3′ end to protect them from serum 3′-exonucleases (12–15).

Microinjected fluorescent ODNs, unlike ODNs added to culture media, do not localize in the cytoplasm but in the nucleus (8, 16). In a time course assay following microinjection, fluorescence attached to phosphodiester ODNs was not retained by the nucleus or the cell (16). This effect was attributed to nuclease degradation of ODNs followed by cellular export of fluorescent metabolites (16). Upon microinjection of ODNs which contained nuclease-resistant modifications, such as phosphorothioate or α-anomeric linkages, nuclear fluorescence persisted for several hours (16). Although the export rates of fluorescent metabolites of the modified ODNs were not evaluated, it was assumed that nuclease stable linkages prevented the dissipation of fluorescence by inhibiting breakdown of the modified ODNs.

The observation that unmodified ODNs are degraded in the nucleus contradicts the conclusions of the cellular uptake/metabolism studies, described above. One explanation for this paradox is that cellular uptake and fractionation experiments measure lysosomal degradation of ODNs, whereas microinjection experiments demonstrate metabolism in the cytoplasm and nucleus. Given this possibility, cytoplasmic and nuclear ODN metabolism needs to be better characterized, since the results will have a profound influence on the design of antisense ODNs.

We developed an indirect assay using fluorescence microscopy to evaluate cellular distribution and degradation of ODNs in live mammalian cells. To eliminate permeability questions, microinjection was used to bypass the lipid bilayer. Fluorescence microscopy has the advantage that it can be done with live cells,

* To whom correspondence should be addressed

+ Present address: Program of Cellular and Developmental Biology, Harvard Medical School, Boston, MA 02115, USA

avoiding potential cell-fractionation artifacts. Since the assumption is that fluorescent metabolites will be exported from the cell, fluorescent ODN metabolites were synthesized and evaluated.

MATERIALS AND METHODS

Monomer reagents

Dimethoxytrityl[DMT]-protected H-phosphonate forms of 2′-deoxy(A, G, C,T) were prepared as described (17). 2′-*O*-allyl T and 5-methyl-2′-*O*-allylcytidine were prepared as the DMT-protected H-phosphonate using standard chemistry (17, 18). 2′-*O*-methyl (2′-*O*-Me) T was also prepared as the DMT-protected H-phosphonate as described (17, 19). *N*-monomethoxytrityl[MMT]-protected aminohexanol H-phosphonate was prepared as described (20). Phosphoramidite forms of 2′-deoxy(A, G, C, T) and 2′-*O*-Me(A, G, C, U) were purchased from Glen Research, Sterling, VA.

Oligonucleotide synthesis

ODNs prepared by the H-phosphonate method were synthesized on an automated synthesizer (model 8750, Milligen Biosearch, Bedford, MA) using standard chemistry on controlled pore glass (CPG) support (17). The ODNs prepared by this method include phosphodiester, phosphorothioate, 2′-*O*-allyl, 2′-*O*-Me T, and phosphoramidate (5′ and/or 3′ end) modifications. Methoxyethylamine (MEA), dodecylamine (C_{12}) and octadecylamine (C_{18}) were used to prepare the phosphoramidate linkages.

ODNs prepared by the phosphoramidite method were synthesized on a Biosearch DNA synthesizer, model 8750, using standard chemistry on CPG support. The ODNs prepared by this method included phosphorothioate, mixed phosphodiester/phosphorothioate, methylphosphonate, and 2′-*O*-Me U, C, A, and G-containing molecules.

ODNs prepared by either chemistry were deprotected and cleaved from support using a modified procedure (21). Briefly, the ODN-CPG was suspended in *t*-butylamine: MeOH: H_2O (1: 1: 1) for 1 hour at 90°C. The supernatant was dried and the ODN was purified (described below).

Fluorescent labelling and purification

All of the ODNs used for fluorescent labelling were prepared with MMT-protected aminohexanol on the 5′ end. Following synthesis, MMT was removed using successive column washes with 2.5% dichloroacetic acid in methylene chloride. The CPG, with the ODN attached, was added to 4 equivalents of the succinimidyl ester of 5-(and 6-) carboxyfluorescein (Molecular Probes, Eugene, OR) or 5-(and 6-) tetramethylrhodamine (Molecular Probes) in 10% diisopropylethylamine in dimethylformamide (dry). The solution was vigorously shaken for 15 hours. Non-coupled fluorophore was removed from the CPG by extensive washing. The fluorescent ODN was detached from the support and deprotected as described above. The fluorescent ODN was next purified from unconjugated ODN on a preparative 20% acrylamide gel and extracted from a gel slice using an overnight incubation in 0.5 M NH_4Cl. Subsequently, the ODN was desalted using a NAP-25 column (Pharmacia, Piscataway, NJ). Finally, a Na^+ exchange was performed on an AG 50W-X8 cation exchange resin (Bio-Rad, Hercules, CA). The ODN was analyzed using analytical HPLC, gel electrophoresis, base composition analysis (22), and UV spectroscopy. Using the above method, there was no evidence of contaminating unconjugated fluorophore in the sample.

Microinjection

For the indicated experiments, either rat embryo fibroblast (Rat2), African green monkey kidney (CV1), mouse embryo fibroblast ($C^3H10T1/2$), human epitheloid carcinoma (HeLa) or human ovarian carcinoma (SK-OV-3) cells were used. All cell lines were purchased from the American Type Culture Collection, Rockville, MD. Rat2 and SK-OV-3 cells were grown in DMEM + 10% FBS; $C^3H10T1/2$, CV1 and HeLa cells were grown in MEM + 10% FBS. Cells were cultured in DMEM + 10% FBS + 50 mM HEPES (pH 7.3) on an inverted microscope (Zeiss Axiovert 10) equipped with a custom made temperature-controlled chamber set at 34°C. Microinjection was performed using a pneumatic controller (Nikon PLI-188) attached to a micromanipulator (Narishige MO-302).

Cells were injected in the cytoplasm approximately 0.5 to 1 nuclear diameters away from the nuclear membrane or, for certain experiments, directly into the nucleus. Cells were injected with fluorescent ODN (50 μM) in 50 mM HEPES (pH 7.3), 90 mM KCl, and 2 mg/ml 10,000 MW fluorescent dextran (Molecular Probes). Approximate injection volumes were 20–40 fl for cytoplasmic injections ($\sim$1/10 the cell volume) and 10–20 fl for nuclear injections ($\sim$1/20 the cell volume; [23]). The injected cells were placed in CO_2 incubators at 37°C prior to microscopy unless they were used for time points immediately following microinjection.

Confocal fluorescence microscopy

A Zeiss Axiovert 10 microscope was attached to a real-time laser confocal video scan module (equipped with a 457, 488, and 529 nm three-line laser, Noran Instruments, Madison, WI). Coverslips, containing the live injected cells, were mounted onto drilled petri dishes using Valap (vaseline: lanolin: paraffin [1: 1: 1]; [24]); cells were incubated on the microscope in DMEM + 10% FBS + 50 mM HEPES (pH 7.3) without phenol red. The cells were analysed with either a 63×plan-apochromat or 100×plan-neofluor oil-phase lens.

Image processing

Images from the confocal microscope were collected by averaging 32–64 frames using a Dage DSP-200 processor. The data were then sent directly into a framegrabber board (Data Translation, Marlboro, MA) installed in a Mac II computer and were stored on a hard disk (640×480 pixel format) or eraseable optical disk.

Background-subtracted images were analyzed for relative fluorescent intensity. The nuclear and total cellular fluorescence in successive confocal slices were determined using Image software (W. Rasband, NIH). The ratio of the fluorescent intensity of the nuclear-localized ODN (fluorescein, unless otherwise indicated) to the nuclear intensity of the 10 kD dextran (Texas Red, unless otherwise indicated) was determined in a time course assay following microinjection. Images were collected at low laser settings to minimize fluorescein photobleaching; the fluorescein image was taken first, followed by the Texas Red image. Standard curves for laser intensity and gain settings were generated to directly compare images taken at different settings. Using predetermined laser and gain settings, there was no detectable bleedthrough of fluorescein to Texas Red or vice-versa. Studies showed that the amount of dextran in the nucleus remained constant throughout the time course of experiments and therefore served as an internal control (data not shown).

Table 1. FL = 5-(and 6-)carboxyfluorescein; TR = 5(and 6-) carboxytetramethylrhodamine; o = phosphodiester; s = phosphorothioate

Compound		Sequence (5'-3')
A		FL-oToAoGoCoToAoAoGoGoCoToCoGoAoCoT
B		TR-oToAoGoCoToAoAoGoGoCoToCoGoAoCoT
C		FL-sTsAsGsCsTsAsAsGsGsCsTsCsGsAsCsT
D		TR-sTsAsGsCsTsAsAsGsGsCsTsCsGsAsCsT
E	T16 diester	FL-oToToToToToToToToToToToToToToT
F	T16 thioate	FL-sTsTsTsTsTsTsTsTsTsTsTsTsTsT
G	T8 diester	FL-oToToToToToToToT
H	T8 thioate	FL-sTsTsTsTsTsTsT
I	T4 thioate	FL-sTsTsTsT
J	5'-4D-4T-3'	FL-oToToToTsTsTsTsT

RESULTS

Disposition of phosphodiester and phosphorothioate oligonucleotides microinjected into cells

Fluorescent phosphodiester ODNs were detected for relatively short periods of time when microinjected into either the cytoplasm or the nucleus of cells. Phosphodiester ODNs were prepared conjugated to fluorescein (Table 1; A; also Fig. 1) or tetramethylrhodamine (Table 1; B) on the 5' end using an aminohexanol linker. ODNs were microinjected into the cytoplasm of Rat2 cells together with a 10 kD dextran-labeled with either Texas Red (for fluorescein ODNs) or fluorescein (for tetramethylrhodamine ODNs). Analysis of the live cells using confocal fluorescence microscopy, showed that the fluorescent ODNs localized in the nucleus within minutes for both fluorescein (Fig. 2a, A) and tetramethylrhodamine ODNs. More than 75% of the nuclear fluorescence disappeared 1 hour after injection (Fig. 2a, A−C) and the fluorescence was undetectable after 24 hours. In contrast, the dextran fluorescence remained unchanged (data not shown). The fluorescein ODN was also microinjected directly into the nucleus together with a 70 kD dextran, which was retained by the nucleus, indicating a nuclear injection. The rate of disappearance of ODN-associated fluorescence was similar to that shown for the cytoplasmic injection. Each of the above results were identical in HeLa, SK-OV-3, CV1 and C^{3}H10T1/2 cell lines.

A fluorescent mononucleotide, 5'-fluorescein-dT, was prepared in order to elucidate the fate of metabolites produced by the degradation of fluorescent ODNs. Upon microinjection into each of the cell lines, the compound was diffusely distributed without discrete nuclear localization (Fig. 2b, A). At 20 minutes post-injection, the fluorescence was no longer detected inside the cell (Fig. 2b, B). The same was true for 5'-tetramethylrhodamine-dT. Nuclear localization, therefore, was dependent on the ODN and was not an artifact of the fluorophore. In addition, the assumption that cells could rapidly export fluorescent ODN metabolites was justified.

Replacement of phosphodiester linkages with nuclease-resistant phosphorothioate bonds significantly enhanced the persistence of fluorescence for microinjected ODNs. Fluorescein and tetramethylrhodamine ODNs containing phosphorothioate linkages were prepared whose base sequences were exactly the same as those used above (Table 1; C, D; also Fig. 1). Following microinjection, fluorescent phosphorothioate ODNs rapidly accumulated in the cell nucleus. Approximately 90% of the fluorescence remained in the nucleus after 6 hours for both the

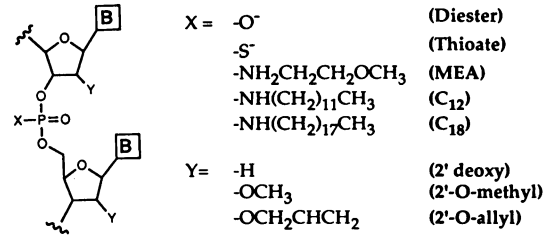

Figure 1. Schematic structure of modifications. B = A, G, C, T, $^{5\text{-me}}$C, or U.

fluorescein- (Fig. 2a, D−F) and tetramethylrhodamine-conjugated phosphorothioate ODNs. A 5'-fluorescein-dT phosphorothioate mononucleotide showed diffuse staining and the fluorescence rapidly disappeared, similar to the result found for the phosphodiester mononucleotide, described above (Fig.2b, A−B). Therefore, the cell rapidly exported a fluorescent phosphorothioate ODN metabolite.

Effects of oligonucleotide length on intracellular persistence of phosphodiester and phosphorothioate oligomers

The rate of disappearance of fluorescence associated with microinjected ODNs depended on ODN length. Following microinjection, both T_8 and T_{16} phosphodiester ODNs (Table 1; G, E, respectively) localized in the nucleus. Subsequently, the total level of fluorescence in the cell rapidly declined. Fluorescein-T_{16} was approximately 10-fold more long-lived in the nucleus than fluorescein-T_8 (Fig. 3). Similarly, fluorescein-T_{16} phosphorothioate (Table 1; F) persisted in the nucleus for a longer time than fluorescein-T_8 phosphorothioate (Table 1; H; Fig. 3); both were substantially more long-lived than the phosphodiesters (Fig. 3).

We studied the process of export of fluorescent phosphorothioate metabolites from the cell. Fluorescence from the fluorescein-T_8 phosphorothioate accumulated in cytoplasmic compartments at 6 hours post-injection, while nuclear fluorescence correspondingly decreased (Fig. 4, D−F). A fluorescein-T_4 phosphorothioate (Table 1; I) behaved similarly; it was exported more rapidly than its T_8 analogue (Fig. 3; Fig. 4, A−C). The identity of the cytoplasmic granules is currently unknown; however, their appearance directly correlates with the dissipation of fluorescent ODN from the nucleus.

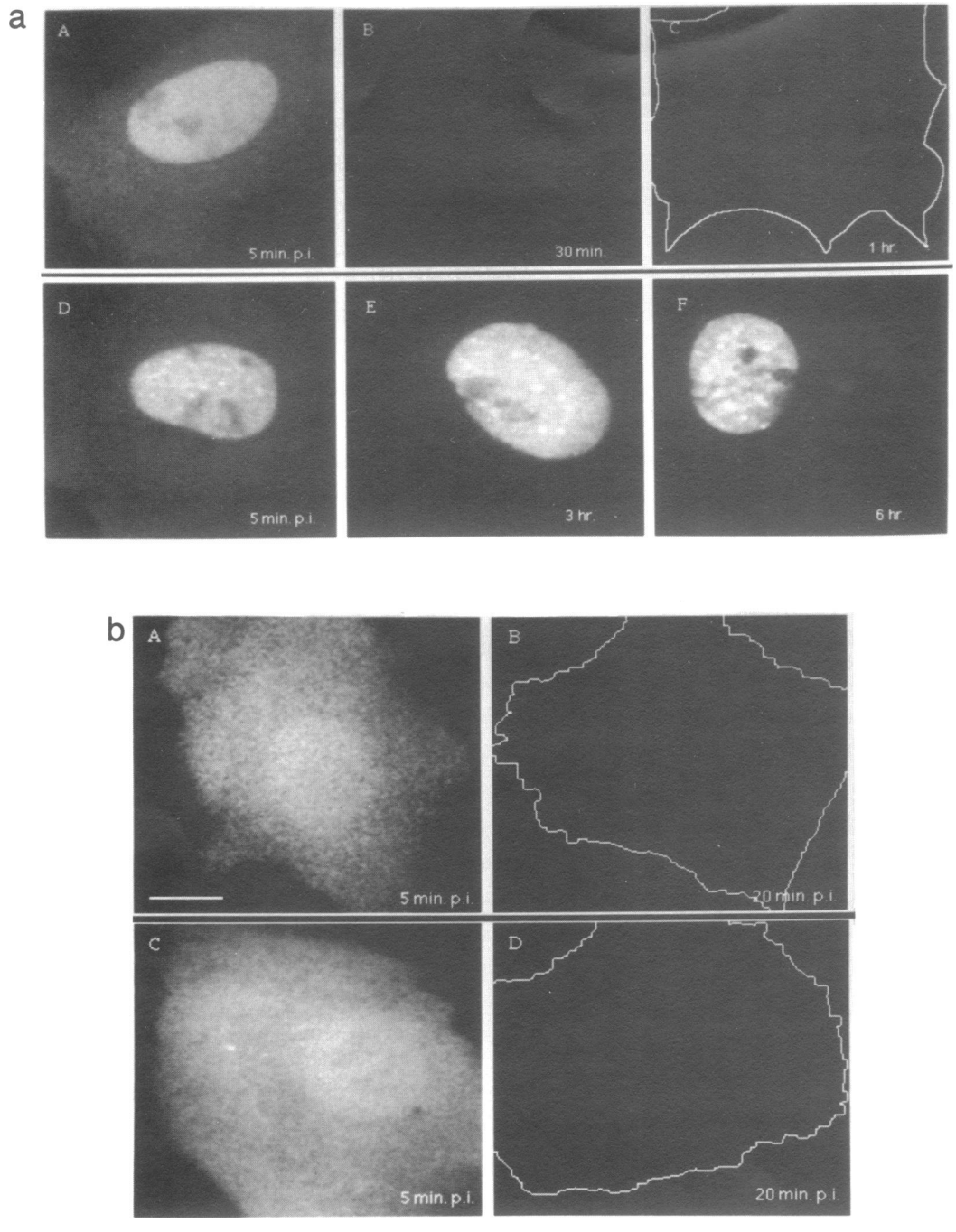

Figure 2. (**a**) Microinjection of fluorescein-labeled phosphodiester or phosphorothioate ODNs. Compounds A and C (phosphodiester or phosphorothioate 16mer, respectively; Table 1) were microinjected, together with a Texas Red-labeled 10 kD dextran, into the cytoplasm of Rat2 cells using a needle concentration of 50 μM of ODN and 2 mg/ml dextran. Live cells were analysed using fluorescence confocal microscopy. Injected cells were identified by the co-injected dextran (not shown). Images were taken at identical settings; background-substracted images were equivalently contrast-enhanced for photography. Panels (A−C), phosphodiester 16mer, 5 min., 30 min., and 1 hr. post-injection (p. i.); panels (D−F), phosphorothioate 16mer, 5 min., 1 hr., and 6 hr. post-injection. White outline in panel C indicates tracing of injected cell. Bar indicates 10 μm. (**b**) Microinjection of fluorescein-labeled phosphodiester or phosphorothioate mononucleotides. 5′-fluorescein-dT mononucleotides were microinjected into the cytoplasm of Rat2 cells at a needle concentration of 50 μM as described above. Panels (A−B), phosphodiester mononucleotide, 5 min. and 20 min. post-injection, respectively; panels (C−D), phosphorothioate mononucleotide, 5 min. and 20 min. post-injection, respectively. White outline in panels A and C indicate tracing of injected cell. Bar indicates 10 μm.

Involvement of 3′-exonuclease in oligonucleotide degradation

Modifications previously found to inhibit 3′-exonuclease digestion did not completely inhibit the rapid export of fluorescence associated with phosphodiester ODNs.

A fluorescein-T_8 ODN was prepared containing four 5′ phosphodiester linkages and four 3′ phosphorothioate linkages (Table 1; J) such that the modifications blocked 3′-exonuclease degradation (14). Following microinjection of this compound into

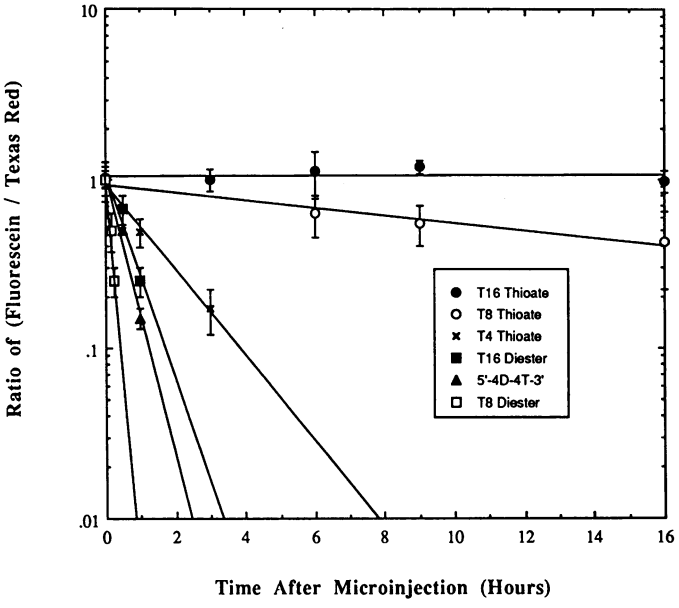

Figure 3. Intracellular stability of poly(T)$_n$ compounds. 20–40 Rat2 cells were microinjected (see figure 2 and methods) with fluorescein-labeled ODN for each time point, of which 5–10 cells were randomly selected for determining the average, relative intracellular concentration of fluorescence. Texas Red-dextran was co-microinjected as an internal control. Data was prepared from background-subtracted images. At least three time points were run per compound in which the ODN fluorescence could be detected above backround. Data in which the ODN fluorescence cannot be detected above backround are not included, although the extrapolation of the curves reflect when the fluorescence reached backround. The fluorescein to Texas Red ratio (see methods) was plotted versus time following injection (hours). Error bars represent one standard deviation of variability of the ratio for the 5–10 cells. Symbols are listed in rank order of relative persistence of ODN fluorescence as follows: ●, T_{16} phosphorothioate (Table 1; F); ○, T_8 phosphorothioate (Table 1; H); x, T_4 phosphorothioate (Table 1; I); ■, T_{16} phosphodiester (Table 1; E); ▲, 5′-T_4 phosphodiester-T_4 phosphorothioate-3′ (Table 1; J), □, T_8 phosphodiester (Table 1; G).

Rat2 cells, fluorescence persisted 5-fold longer than fluorescence associated with the unmodified T8 phosphodiester ODN. This result implicates an intracellular 3′-exonuclease activity in the nucleus. However, the fluorescent half-life of the pure T_8 phosphorothioate ODN was more than 30-fold longer than the phosphorothioate/phophosphodiester chimera (Fig. 3).

Another modification shown to inhibit 3′-exonuclease degradation of a phosphodiester ODN was substitution of two 3′ terminal linkages with MEA (see Fig. 1; [14]). This modification did not prolong the persistence of fluorescence of fluorescein-T_8 phosphodiester ODNs (Fig. 5). Mixed-sequence phosphodiester ODNs (18 nucleotides long) synthesized with either fluorescein or tetramethylrhodamine on the 5′ end and two MEA linkages on the 3′ end behaved similarly (data not shown).

Two other phosphoramidate modifications which incorporate longer alkyl moieties on the 3′ end were evaluated. Fluorescein-T_8 phosphodiester ODNs, made with either two 3′ terminal C_{12}- or C_{18}-phosphoramidate modifications (see Fig. 1), localized in the cytoplasm rather than in the nucleus; this effect was more marked with the longer carbon chain (Fig. 5). The site of injection affected the half-life of these ODNs, suggesting that nuclease activity may vary between cellular compartments. When the C_{18}-modified ODN was microinjected directly into the nucleus, a majority of the material remained nuclear-localized, but the fluorescence disappeared more rapidly than when injected into the cytoplasm. It appears that either nuclease activity, though still present in the cytoplasm, is low, or sequestration in cytoplasmic organelles partially protects the ODN from nucleases.

Various modifications to the 3′ end of ODNs with a variety of modifications do not lead to the increased cellular retention of fluorescence observed with the pure phosphorothioate T_8 ODN. While 3′-exonuclease is detected, 5′-exonuclease and/or endonuclease activities are likely to be responsible for the cleavage of the phosphodiester linkages in the compounds

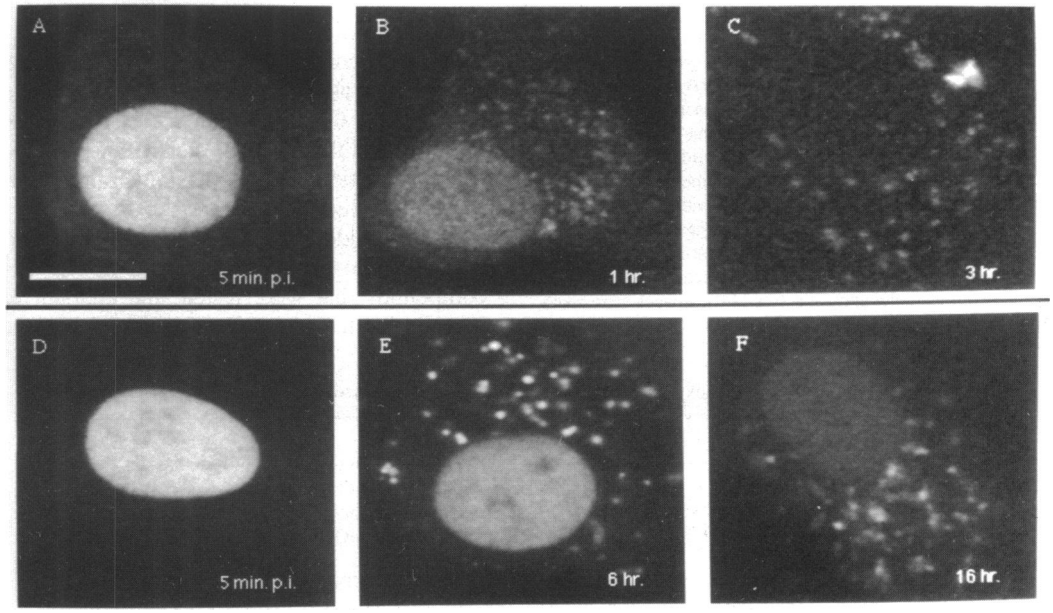

Figure 4. Export of T_4 and T_8 phosphorothioate ODNs (Table 1; I, H, respectively). The T_4 and T_8 phosphorothioate ODNs were microinjected into Rat2 cells as described in Figure 1. Live cells were viewed and images were captured as described in Figure 1 and in the methods. Panels (A–C): T_4, 5 min., 1 hr., and 3 hr. post-injection, respectively; panels (D–F): T_8, 5 min., 6 hr., and 16 hr. post-injection, respectively. Bar indicates 10 μm.

described above (25, 26). These activities exist in both the cytoplasm and nucleus.

Endonuclease is detected in somatic cells

In order to assess the presence of intracellular endonuclease activities, chimeric ODNs were synthesized such that phosphodiester linkages were flanked by four phosphorothioates on the 5′ end (including the 5′-fluorescein-aminohexanol moiety) and by a varied number of phosphorothioates on the 3′ end (Table 2). Thus, the nuclease-sensitive phosphodiester linkages were protected on the ends from 3′- and 5′-exonucleases, but not endonucleases.

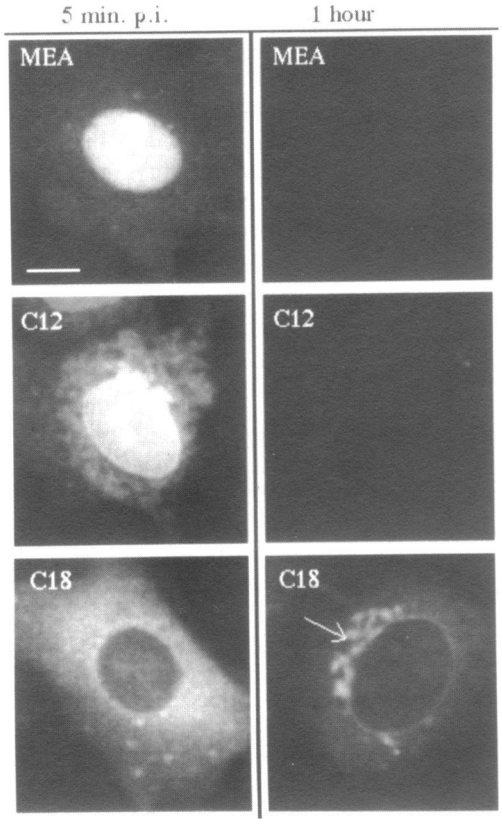

Figure 5. Distribution and degradation of 3′ modified T_8 ODNs. T_8 phosphodiester ODNs modified at the two 3′ terminal internucleotide linkages with MEA, C_{12}-phosphoramidates, or C_{18}-phosphoramidates were microinjected into the cytoplasm of Rat2 cells and viewed live using fluorescence microscopy at 0 or 1 hour post-injection. The fluorescence pattern for each of these ODNs is distinct. The MEA containing ODN localizes in the nucleus, indistiguishable from unmodified ODNs. For the C_{12}-phosphoramidate containing oligonucleotide, a reticular structure in the cytoplasm is stained, as well as the nuclear envelope, suggesting that the compound is associating with the endoplasmic reticulum (see [43]). For the C_{18}-phosphoramidate containing oligonucleotide, the fluorescence is diffuse in the cytoplasm at 5 minutes post-injection, and by one hour the fluorescence accumulates in a perinuclear localization (arrow), characteristic of associating with the golgi apparatus (see [44]). Images were taken as described in Figure 1 and in the methods. Bar indicates 10 μm.

The assumption for the assay was that endonuclease cleavage, at the phosphodiester positions, would liberate the fluorescein-tetramer phosphorothioate which would subsequently be exported from the cell. We had previously observed that fluorescently-labeled phosphorothioate tetramers had been exported rapidly from the cell. This was also true for the TAGC (Table 2; N) phosphorothioate ODN (Fig. 6A). Therefore, the rate of export of the tetramers was sufficiently more rapid than that of the parent ODNs; this allowed us to test for endonuclease activity.

Fluorescein-labeled phosphorothioate ODNs (16 nucleotides, mixed sequence) containing either 2, 4 or 6 internal phosphodiester linkages were synthesized (Table 2; K, L, M, respectively). Upon microinjection of the chimeric compounds into Rat2 cells, nuclear localization was rapid; at later time points, cytoplasmic granules began to appear. The rate of appearance of fluorescent cytoplasmic granules was proportional to the number of phosphodiesters in the compound and directly reflected the decrease of nuclear fluorescence (Fig. 6A). Similar results were obtained with CV1, HeLa, $C^3H10T1/2$ and SK-OV-3 cells.

An MEA/phosphodiester chimeric ODN was prepared of analogous design to the phosphorothioate containing six internal phosphodiester linkages (MEA/diester/MEA; Table 2; R). A tetramer MEA (Table 2; Q) and a 16 nucleotide MEA (Table 2; S) compound were also synthesized as controls. Five minutes after microinjection into Rat2 cells, each of these three compounds partitioned between the nucleus and the cytoplasm in a 60:40 ratio (determined by comparing slice/slice intensities); this distribution pattern was unique to multiple MEA modifications since it was not observed with the phosphodiester ODNs containing two MEA moieties on the 3′ end (see Fig. 5). Intracellular fluorescence associated with the MEA/diester/MEA compound (Table 2; R) had the same half-life following injection as its phosphorothioate analogue (Table 2; M). The half-life of fluorescence associated with the fully-substituted MEA ODN was longer (Fig. 6B). Fluorescence associated with both the MEA tetramer and the MEA/diester/MEA 16mer showed the pattern of redistribution into cytoplasmic granules which paralleled loss of cellular fluorescence.

We conclude that endonuclease, present in mammalian cells, degrades phosphodiester linkages in ODNs. For the chimeric compounds that were tested, the endonuclease appears to be specific for the internally substituted phosphodiester linkages.

Table 2. FL = 5-(and 6-)carboxyfluorescein; s = phosphorothioate, o = phosphodiester; x = MEA

Compound		Sequence (5′-3′)
K	2 diester	FL-sTsAsGsCoToAsAsGsGsCsTsCsGsAsCsT
L	4 diester	FL-sTsAsGsCoToAoAoGsGsCsTsCsGsAsCsT
M	6 diester	FL-sTsAsGsCoToAoAoGoGoCsTsCsGsAsCsT
N	4 thioate	FL-sTsAsGsC
O		FL-sTsAsGsToToToToTsTsTsTsCsGsAsCsT
P		FL-sTsAsGsCoCoCoCoCsCsCsTsCsGsAsCsT
Q	MEA4	FL-xTxAxGxC
R	MEA/D/MEA	FL-xTxAxGxCoToAoAoGoGoCxTxCxGxAxCxT
S	MEA16	FL-xTxAxGxCxTxAxAxGxGxCxTxCxGxAxCxT

Modified sugar moieties confer intracellular nuclease resistance

Substitution at the 2′-ribose position of ODNs with *O*-alkyl derivatives had previously resulted in enhanced stability *in vitro* to various nucleases and cellular extracts (18, 19, 27). 5′-fluorescein T_8 phosphodiester ODNs containing either 2′-*O*-methyl (2′-*O*-Me) or 2′-*O*-allyl derivatives of T were prepared (see Fig. 1). Each of these ODNs localized in the nucleus within 5 minutes after microinjection. The 2′-substitutions significantly stabilized nuclear fluorescence associated with microinjected phosphodiester ODNs (Fig. 7). The 2′-*O*-allyl modification resulted in an 8-fold increase in stability compared to the *O*-methyl T_8 derivative and a 60-fold increase in stability compared to the 2′-deoxy T_8 phosphodiester ODN (Fig. 7). Other sequences tested with similar results included 2′-*O*-Me C_8, 2′-*O*-Me A_8 and 2′-*O*-allyl (T $^{5\text{-me}}C)_4$.

5′-fluorescein-2′-*O*-allyl $(T)_4$ was also injected; its half-life in the cell was one hour, much shorter than that of the T_8 2′-*O*-allyl ODN (Fig. 7). Finally, a 5′-fluorescein-2′-*O*-allyl T mononucleotide was injected. The distribution of fluorescence associated with this compound was diffuse rather than nuclear localized; the fluorescence disappeared from the cell within 15 minutes post-injection.

Taken together, these results suggest that the fates of metabolites of 2′-modified ODNs are similar to those of

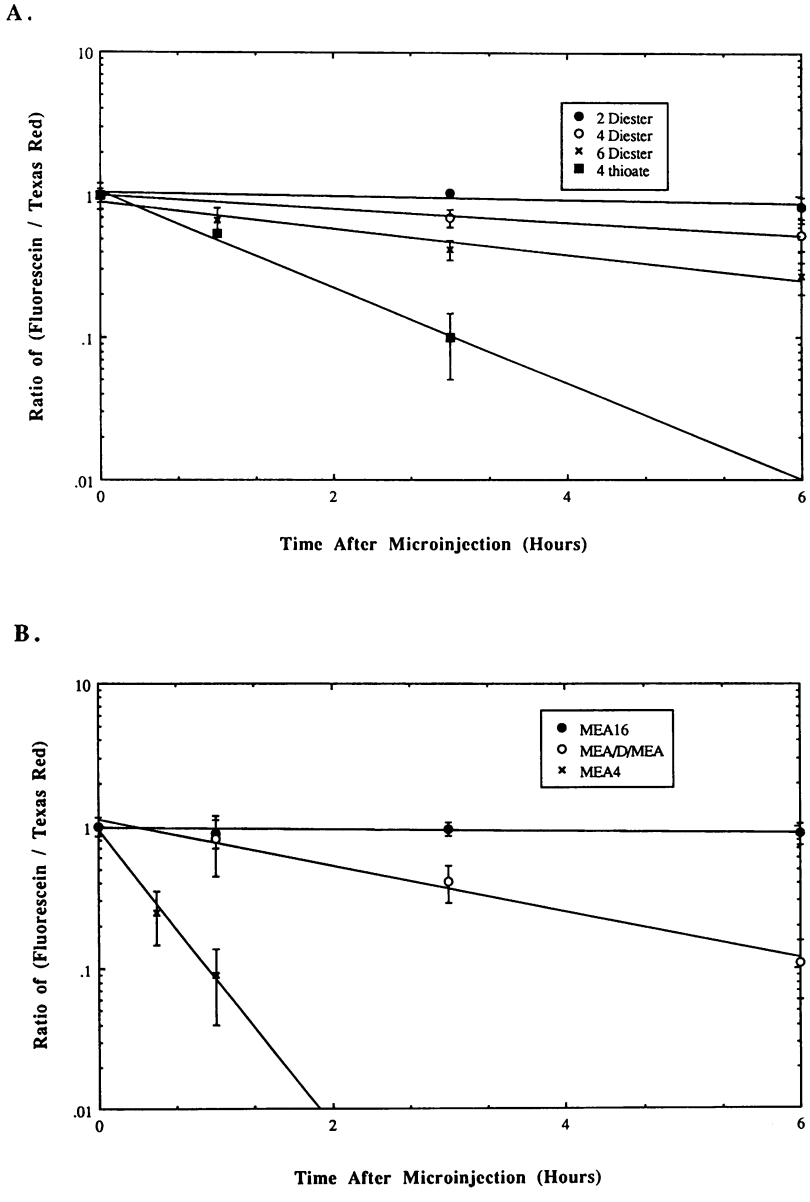

Figure 6. Detection of intracellular endonuclease activity. Compounds were microinjected into Rat2 cells as described in figure 1. Data were obtained as described in Figure 2. Either phosphorothioate ODNs were synthesized with internal substituted phosphodiesters (A) or MEA ODNs were synthesized with internal phosphodiesters (B). (**A**) In rank order of relative fluorescence persistence: ●, 2 internal phosphodiesters (Table 2; K); ○, 4 internal phosphodiesters (Table 2; L); **x**, 6 internal phosphodiesters (Table 2; M); ■, phosphorothioate tetramer (Table 2; N). (**B**) In rank order of relative stability: ●, 16mer MEA (Table 2; S); ○, 6 internal phosphodiesters (MEA/Diester/MEA; Table 2; R); **x**, MEA tetramer (Table 2; Q).

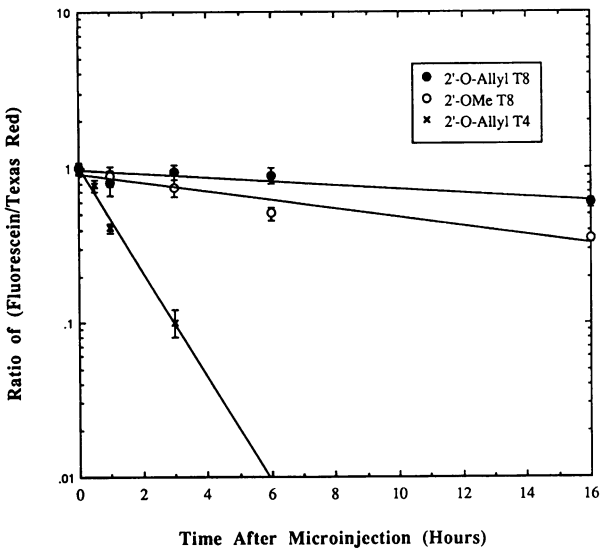

Figure 7. Stabilization of ODNs by substitution at the 2'-ribose position. Compounds were microinjected as described in figure 1 into Rat2 cells. Data were obtained as described in Figure 2. ●, 2'-*O*-allyl T_8; ○, 2'-*O*-Me T_8; x, 2'-*O*-allyl T_4.

unmodified analogues, and thus the increased half-life in the nucleus of the fluorescent 2'-*O*-allyl T_8 ODN reflects its insensitivity to nuclease.

DISCUSSION

Using an indirect fluorescence-based assay, we have demonstrated the presence of nucleases in the cytoplasm and nucleus of live cells. We make five conclusions from our findings: (*i*) Export of fluorescent ODN metabolites from the nucleus and cytoplasm is sufficiently rapid that an indirect assay can be used to measure ODN stability in live cells. (*ii*) The export of fluorescence occurs regardless of the cell line or the fluorophore. (*iii*) Fluorescence associated with fluorescently-labeled phosphodiester ODNs microinjected into somatic cells initially localizes in the nucleus, then dissipates with a half-life of approximately 15−30 minutes; this result is likely a result of nuclease degradation followed by export of fluorescent metabolites. (*iv*) The proposed nuclease activities include 3'-exonuclease and endonuclease; the presence of 5'-exonuclease was not explored. (*v*) Intracellular nuclease resistance is conferred by MEA or phosphorothioate linkages or 2'-*O*-allyl substitutions on ribose. Cell extracts were previously shown to contain nuclease activities (25) including endonuclease (26). Our studies confirm that such activities exist in the cellular compartments in which ODNs accumulate after microinjection. Furthermore, these nucleases can degrade micromolar levels of nuclear-localized ODNs containing phosphodiester bonds. It is important to note that these conclusions have been generalized based on the limited number of sequences tested.

We have observed the redistribution of fluorescent ODNs using fluorescence microscopy. Presumably, part of the reduction of fluorescence, following ODN degradation, is due to diffusion or organic anion transporters (28). Many of the fluorescent metabolites we evaluated seem to be autophaged in some fashion and exocytosed; this is a proposed mechanism for cellular RNA degradation (see 29−31). The process is sequence-independent, since it was observed for both T_4 and TAGC phosphorothioate tetramers; also, the process is not dependent on the presence of polyanions or deoxyribose sugars, since it was observed with both MEA-containing compounds and 2'-*O*-allyl compounds. It is possible that localization of fluorescent ODN metabolites into the cytoplasmic granules simply represents areas of the cell where the fluorescence is protected from export. In addition, it is possible that other factors may be responsible for the decrease in fluorescent intensity, such as intracellular quenching. In all cases, the strong dependence of fluorescence disappearance on ODN chemistry and length supports nuclease degradation of the ODNs as the mechanism preceding fluorescent loss.

The presence of intracellular endonuclease introduces significant challenges for developing potent antisense ODNs. Unmodified, 3' modified, and 5'/3' modified ODNs which contain phosphodiester linkages, are not likely to be very potent inhibitors. MEA modifications on the 5' and 3' ends of phosphodiester ODNs prevented endonuclease attack in *Xenopus* eggs and embryos (32, 33). The endonuclease activity in mammalian cells, however, must differ from that identified in *Xenopus* embryos, since it is not blocked by 5' and 3' MEA linkages. In contrast, ODNs containing complete backbone modifications, such as phosphorothioate ODNs, are likely to have the most potent effects.

There has been some controversy in the antisense field regarding the intracellular fate of oligonucleotides when they are added to cells. Previously, cell fractionation studies had concluded that ^{32}P-labeled phosphohodiester ODNs, added to HeLa cells in culture media, localize in the nucleus and are stable for more than four hours (12, 13). However, our data show that nuclease activities rapidly degrade fluorescently-labeled phosphodiester ODNs in HeLa cell nuclei (unless they are modified on the ribose ring). Previous studies too have shown endocytic compartmentalization of fluorescent ODNs with no nuclear accumulation (8, 9; R. Wagner, unpublished results) unless cell permeabilization reagents are used (5, 6). We believe that the discrepancy between these results is due to the inherent problems with cell fractionation in which organelles, including endosomes and lysosomes, contaminate the nuclear fraction by as much as 50% during fractionation and centrifugation (34). It is therefore inherently difficult to isolate pure subcellular fractions, and the potential for artifacts is high. We would predict that if phosphodiester oligonucleotides escaped their lysosomal fate, they would be rapidly degraded; if phosphorothioate oligonucleotides escaped, they would remain in the nucleus, relatively undegraded. These hypotheses are supported by experiments in which cell permeabilization reagents have been utilized. When used in combination with the cell permeabilization reagent lipofectin, fluorescently-labeled phosphorothioate ODNs are released from granular compartments and migrate to the nucleus, where the fluorescence persists (5). In contrast, when fluorescently-labeled phosphodiester oligonucleotides are treated the same way, fluorescence in the nucleus is not detectable which is likely the result of nuclease degradation (R. Wagner, unpublished results). Thus, our results are consistent with the model that fluorescently-labeled ODNs show very poor permeability to the nucleus when added to cells unless cell permeabilization reagents are utilized.

We have started to extrapolate from our conclusions to the design of antisense reagents. Several ODN modifications have been previously developed which optimize nuclease stability while retaining the ability to recruit RNase H when bound to RNA.

For example, phosphorothioate, MEA/diester hybrids (32, 33), or methylphosphonate/diester hybrids (35) have each been useful for recruiting RNase H when bound to RNA (32, 36–38). However, each of these modified internucleotide linkages decrease the affinity of ODNs for RNA (39). Non-RNase-H-mediated inhibition of gene expression may be an additional potent antisense mechanism, presumably requiring both nuclease resistance and high affinity for RNA. As a model series, we have evaluated ODNs substituted at the 2′-ribose position. These modifications were previously demonstrated *in vitro* to have higher affinity for RNA compared to unmodified ODNs (40), as well as stability *in vitro* to various RNases and DNases (18). We have shown that the fluorescently-labeled 2′-*O*-allyl substituted ODNs are more stable in live cells than the 2′-*O*-Me derivative and are greater than 60-fold more stable than 2′-deoxy oligonucleotides. Given the potential of 2′-*O*-allyl ODNs to bind intracellular RNA (41, 42), it will be interesting to evaluate this new class of compounds in gene inhibition experiments.

In summary, a series of backbone structural modifications were shown to dramatically affect the distribution and metabolism of fluorescently-labeled ODNs within live cells. ODNs composed of most chemistries showed significant nuclear accumulation following injection; however, C_{12}- and C_{18}-phosphoramidate modifications resulted in cytoplasmic localization. Intracellular nucleases likely account for the majority of ODN metabolism following injection; nucleolytic degradation of ODNs can be prevented by using either internucleotide linkage substitutions, such as phosphorothioate and phosphoramidate, or 2′-ribose substitutions, such as 2′-*O*-allyl.

Antisense gene inhibition offers great promise, but technical challenges remain. Intracellular nucleases are a major hurdle for antisense development; however, their identification leads to significant progress in developing the most potent inhibitors.

ACKNOWLEDGMENTS

We thank Daniel Chin for continued discussion, microinjection and microscopy training, and expert advice. Also, we thank Mark Matteucci and Jay Toole for critical discussions and Megan Williams for editing assistance. This research was supported in part by the Defense Advanced Research Projects Agency.

REFERENCES

1. Bischofberger, N., and Wagner, R.W. (1992) *Seminars in Virology* **3**, 57–66.
2. Goodchild, J. (1990) *Bioconjugate Chem.* **1**, 165–187.
3. Hélène, C., and Toulmè, J-J. (1990) *Biochim. et Biophys. Acta* **1049**, 99–125.
4. Riordan, M.L., and Martin, J.C. (1991) *Nature* **350**, 442–443.
5. Bennett, C.F., Chiang, M.-Y., Chan, H., Shoemaker, J.E.E., and Mirabelli, C.K. (1992) *Mol. Pharm.* 41, 1023–1033.
6. Thierry, A.R., and Dritschilo, A. (1992) *Nucleic Acids Res.* **20**, 5691–5698.
7. Gao, W.-Y., Storm, C., Egan, W., and Cheng, Y.-C. (1993) *Mol. Pharm.* 43, 45–50.
8. Chin, D.J., Green, G.A., Zon, G., Szoka, Jr., F.C., and Straubinger, R.M. (1990) *The New Biologist* **2**, 1091–1100.
9. Loke, S.L., Stein, C.A., Zhang, X.H., Mori, K., Nakanishi, M., Subasinghe, C., Cohen, J.S., and Neckers,L.M. (1989) *Proc. Natl. Acad. Sci. USA* **86**, 3474–3478.
10. Holt, J.T., Redner, R.L., and Nienhuis, A.W. (1988) *Mol. Cell. Biol.* **8**, 963–973.
11. Wickstrom, E.L., Bacon, T.A., Gonzalex, A., Freeman, D.L., Lyman, G.H., and Wickstrom, E. (1988) *Proc. Natl. Acad. Sci. USA* **85**, 1028–1032.
12. McShan, W.M., Rossen, R.D., Laughter, A.H., Trial, J., Kessler, D.J., Zendeui, J.G., Hogan, M.E., and Orson, F.M. (1992) *J. Biol. Chem.* **267**, 5712–5721.
13. Postel, E.H., Flint, S.J., Kessler, D.J., and Hogan, M.E. (1991) *Proc. Natl. Acad. Sci. USA* **88**, 8227–8231.
14. Shaw, J.P., Kent, K., Bird, J., Fishback, J., and Froehler, B. (1991) *Nucleic Acids Res.* **19**, 747–750.
15. Gamper, H.B., Reed, M.W., Cox, T., Virosco, J.S., Adams, A.D., Gall, A.A., Scholler, J.K., and Meyer, Jr., R.B. (1993) *Nucleic Acids Res.* 21, 145–150.
16. Leonetti, J.P., Mechti, N., Degols, G., Gagnor, C., and Lebleu, B. (1991) *Proc. Natl. Acad. Sci. USA* **88**, 2702–2706.
17. Froehler, B., Ng, P., and Matteucci, M. (1986) *Nucleic Acids Res.* **14**, 5399–5467.
18. Iribarren, A.M., Sproat, B.S., Neuner, P., Sulston, I., Ryder, U., and Lamond, A.I. (1990) *Proc. Natl. Acad. Sci. USA* **87**, 7747–7751.
19. Sproat, B.S., Lamond, A.I., Beijer, B., Neuner, P., and Ryder,U. (1989) *Nucleic Acids Res.* **17**, 3373–3386.
20. Sinha, N.D., and Cook, R.M. (1988) *Nucleic Acids Res.* **16**, 2659–2669.
21. Woo, S.L., Menchen, S.M., and Fung, S. (1990) U.S. patent #4,965,349.
22. Eadie, J.S., MacBride, L.J., Efcavitch, J.W., Hof, L.B., and Cathcart, R. (1987) *Anal. Biochem.* **165**, 442–447.
23. Graessmann, M., and Graessmann, A. (1983) *Methods in Enzym.* **101**, 482–492.
24. Swanson, S. (1989) *Methods in Cell Biol.* **29**, 137–151.
25. Furdon, P.J., Dominski, Z., and Kole, R. (1989) *Nucleic Acids Res.* **17**, 9193–9204.
26. Hoke, G.D., Draper, K., Freier, S.M., Gonzalex, C., Driver, V.B., Zounes, M.C., and Ecker, D.J. (1991) *Nucleic Acids Res.* **19**, 5743–5748.
27. Cotten, M., Oberhauser, B., Brunar, H., Holzner, A., Issakides, G., Noe, C.R., Schaffner, G., Wagner, E., and Birnstiel, M.L. (1991) *Nucleic Acids Res.* **19**, 2629–2635.
28. Steinberg, T.H., Newman, A.S., Swanson, J.A., and Silverstein, S.C. (1987) *J. Cell Biol.* **105**, 2695–2702.
29. Heydrick, S.J., Lardeux, B.R., and Mortimore, G.E. (1991) *J. Biol. Chem.* **266**, 8790–8796.
30. Lardeux, B.R., and Mortimer, G.E. (1987) *J. Biol. Chem.* 262, 14514–14519.
31. Seglen, P.O., Gordon, P.B., and Holen, I. (1990) *Seminars in Cell Biol.* **1**, 441–448.
32. Dagle, J.M., Walder, J.A., and Weeks, D.L. (1990) *Nucleic Acids Res.* **18**, 4751–4757.
33. Dagle, J.M., Walder, J.A., and Weeks, D.L. (1991) *Antisense Res. and Dev.* **1**, 11–20.
34. Howell, K.E., Devaney, E., and Gruenberg, J. (1989) *Trends Biol. Sci.* **14**, 44–47.
35. Baker, C., Holland, D., Edge, M., and Colman, A. (1990) *Nucleic Acids Res.* **18**, 3537–3543.
36. Agrawal, S., Mayrand, S.H., Zamecnik, P.C., and Pederson, T. (1990) *Proc. Natl. Acad. Sci. USA* **87**, 1401–1405.
37. Quartin, R.S., Brakel, C.L., and Wetmur, J.G. (1989) *Nucleic Acid Res.* **17**, 7253–7262.
38. Stein, C.A., Subasinghe, C., Shinozuka, K., and Cohen, J.S. (1988) *Nucleic Acids Res.* **16**, 3209–3221.
39. Froehler, B., Ng, P., and Matteucci, M. (1988) *Nucleic Acids Res.* **16**, 4831–4839.
40. Inoue, H., Hayase, Y., Imura, A., Iwai, S., Miura, D., and Ohtsuka, E. (1987) *Nucleic Acids Res.* **15**, 6131–6148.
41. Carmo-Fonseca, M., Pepperkok, R., Carvalho, M.T., and Lamond, A.I. (1992) *J. Cell Biol.* **117**, 1–14.
42. Carmo-Fanseca, M., Pepperkok, R., Sproat, B.S., Ansorge, W., Swanson, M.S., and Lamond, A.I. (1991) *EMBO J.* **10**, 1863–1873.
43. Pagano, R.E., and Longmuir, K.J. (1985) *J. Biol. Chem.* **260**, 1909–1916.
44. Pagano, R.E., and Martin, O.C. (1988) *Biochem.* **27**, 4439–4445.